nature communications

Article

https://doi.org/10.1038/s41467-024-52042-w

Aggregation-induced C–C bond formation on an electrode driven by the surface tension of water

Received: 15 March 2024

Accepted: 23 August 2024

Published online: 30 August 2024

Check for updates

Mengfan Li[1] & Xu Cheng[1]

Electrochemical organic synthesis is typically conducted in organic media. The solvent and related supporting electrolytes negatively affect the greenness of electrosynthesis. In this work, with 100% water used as the solvent, we realize aggregation-driven electrochemical radical cross coupling of unsaturated compounds driven by water tension. A key finding is that aggregation of the substrate at the electrode confined the radical intermediate and prevented side reactions, thus providing a way to regulate radical reactions in addition to their native properties. The reaction provides up to 90% yields with almost quantitative chemoselectivity. The pure water system readily yields the products via cold filtration, and the solvent is recycled repeatedly. In particular, the life span of the radical species generated in the reaction increase significantly because of the confined environment in the aggregation state. The greenness of this protocol is further enhanced with readily separation of product from media using cooling and filtration.

Aggregation-driven effects have been extensively studied for use in building optical materials and biomaterials[1,2]. Typically, in aqueous media, aggregation of hydrophobic compounds results in distinct photo-properties. In electrochemical organic syntheses, however, aggregation is not a useful phenomenon. Since mass transfer is frequently a key factor[3,4], organic solvents are the most commonly applied media used to produce homogenous solutions[5–10]. Therefore, if water is used, an organic cosolvent[11–15] or surfactant[16,17] is typically necessary to prevent aggregation of the organic substrate. This micellar system in aqueous media has been established as an efficient protocol in electrochemical synthesis[18–20]. On the other hand, in the absence of phase transfer reagent, hydrophobic compounds aggregate due to their immiscibility, which creates a multiphase system and precludes efficient mass transfer. Therefore, fully aqueous electrochemical organic syntheses are limited[21–25], and the aggregation-driven effect is overlooked in electro-organic synthesis.

On the other hand, multiphase systems could have multiple advantages in electrochemical syntheses, as reviewed by Marken and Wadhawan[26] and Kobayashi[27] We outlined a comparison of electrochemical reactions in organic solvents and aggregation of a substrate on an electrode driven by the water tension[28]. In a homogeneous solution, the concentration of the substrate localized at the electrode is limited and decreases as the reaction proceeds (Fig. 1a). In contrast, an electrode with a large surface/weight ratio, for example, graphite felt (ca. 0.2 m^3/g)[29], provides a lipophilic space for aggregation of organic substrates that would otherwise be suspended in water. Electron transfer between the electrode and the aggregated substrate is facilitated (Fig. 1b). If another water-soluble reactant forms a bond with the reduced substrate, the product will have better solubility and diffuse into the aqueous medium, leaving vacancy for substrate (vide infra). This reaction design uses pure water as the solvent with the on-water-catalysis strategy[30,31] and has substantial advantages (Fig. 1c). First, aggregation provides a confined space for the radical intermediate[32–34], regulating the reactivity of the radical beyond its intrinsic kinetics[35,36]. Second, the starting material remains concentrated at the electrode, which facilitates conversion. Third, a counterreaction, for example, the reduction or oxidation of water, occurs readily, which precludes the need external oxidants or reductants. All of these factors can ensure chemoselectivity, reduce the energy input, and achieve fast conversions. With this model, we report

[1]State Key Laboratory of Coordination Chemistry, Institute of Chemistry and Biomedical Sciences, Jiangsu Key Laboratory of Advanced Organic Materials, School of Chemistry and Chemical Engineering, Nanjing University, Nanjing, China. e-mail: chengxu@nju.edu.cn

https://doi.org/10.1038/s41467-024-52042-w

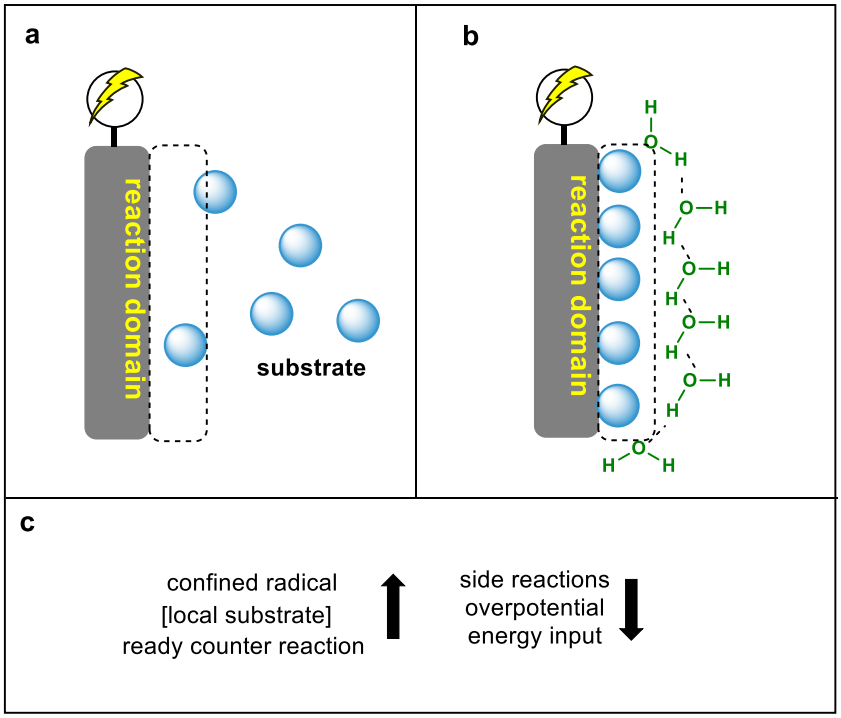

Fig. 1 | Outline of aggregation-driven electrochemical syntheses in aqueous media. a The distribution of substrate in homogenous solution around electrode. **b** The proposed distribution of substrate in aqueous media. **c** The advantages of aggregation-driven electrosynthesis.

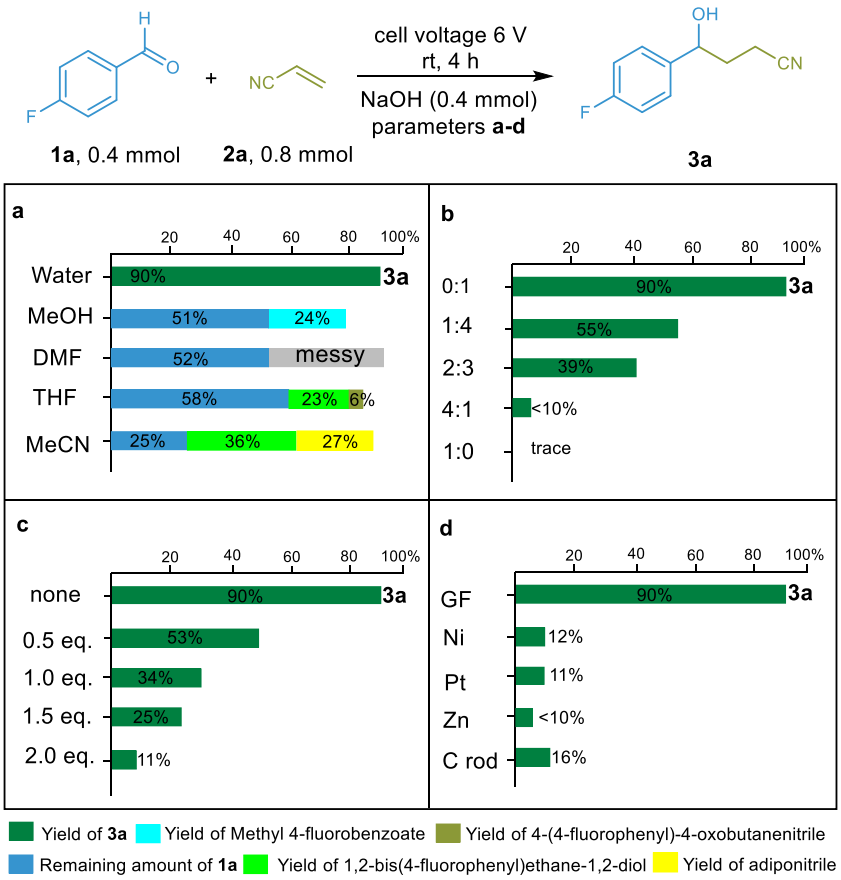

Fig. 2 | ^{1}H NMR analyses of product yields with various reaction parameters. **a** Reaction in different solvents (5 mL) with a graphite felt anode and cathode. **b** Reaction in cosolvent H_2O/MeCN (5 mL) with a graphite felt anode and cathode. **c** Surfactant was used in 5 mL of water with a graphite felt anode and cathode. **d** Water (5 mL), graphite felt anode and other electrode as the cathode.

https://doi.org/10.1038/s41467-024-52042-w

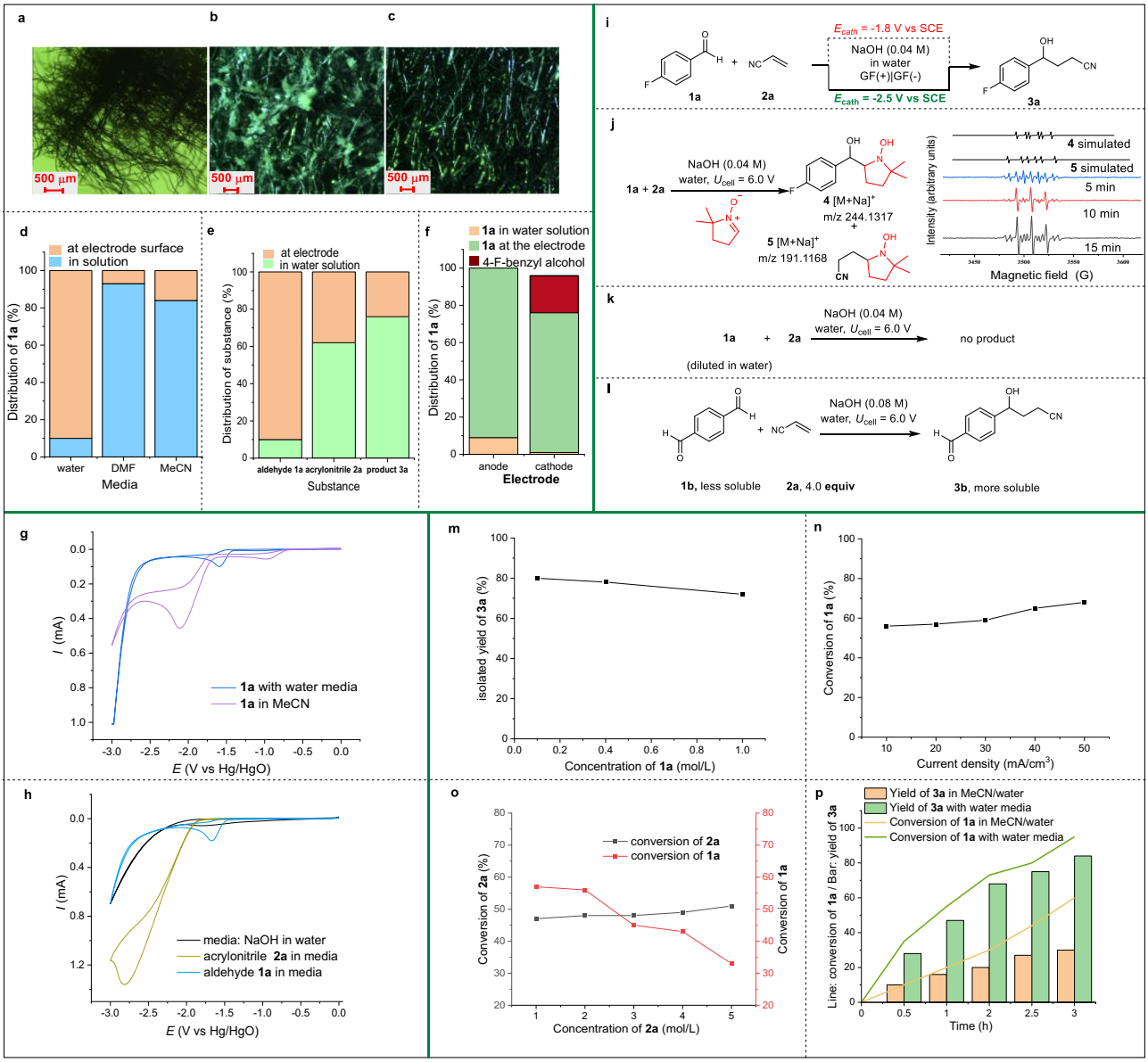

Fig. 3 | Experiments used to elucidate the aggregation effect with aqueous media. a The image of net cathode. **b** The image of aggregated state of substrate **1a** on graphite felt cathode in aqueous media under standard conditions. **c** The image of graphite cathode in reaction of **1a** under standard conditions in MeCN. **d** Mass distribution of **1a** between solvent and aggregation on electrode in different solvents. **e** Mass distribution of compounds between water and aggregation on electrode. **f** Mass distribution of **1a** between water and aggregation on graphite felt anode and cathode in reaction with water as solvent **g** CV analyses of **1a** in different solvents. (Pt(+)|Glassy carbon(-)|Hg/HgO ref, 50 mV/s, solute 0.04 mol/L in 0.1 M NaOH or MeCN). **h** CV analyses of **1a** and **2a** in water (Pt(+)|Glassy carbon(−)|Hg/HgO ref, 50 mV/s, solute 0.04 mol/L in 0.1 M NaOH). **i** Reaction of **1a** and **2a** under controlled cathodic potential. **j** Trapping radicals in the reaction mixture. **k** Result from highly diluted homogenous aqueous solution of **1a**. **l** reaction of substrate **1b** involving double reactive sites. **m** The influence of **1a** on the yield of **3a**. **n** The influence of current density on the conversion of **1a**. **o** The influence of **2a** on the conversions of **1a** and **2a**. **p** The conversion and chemoselectivity in varied solvents.

the formation of distinct electrochemical C–C bonds between unsaturated compounds induced by aggregation in pure water.

Results

A reaction employing aldehyde **1a** and acrylonitrile **2a** was used to compare the outcomes obtained from water-driven aggregation and from a homogeneous solution in an organic solvent (Fig. 2). Water was found to be the optimum medium for achieving the desired conversion (Fig. 2a). The reaction furnished a 90% ^{1}H NMR yield with almost quantitative chemoselectivity. The organic solvent resulted in oxidation of the aldehyde (MeOH) and a very messy mixture (DMF). In THF, the conversion rate was low, and the dimer of **1a** was the major product. In MeCN, electrolysis led to dimerization of **1a** to pinacol in 36% yield, dimerization of acrylonitrile to adiponitrile, and a 25% recovery of aldehyde **1a**. Furthermore, the water was essential for high conversions and chemoselectivities (Fig. 2b). Even the use of 20% MeCN as the cosolvent decreased the yield of product **3a** to 55%. A homogeneous solution of MeCN/water (4:1) afforded **3a** in only 10% yield along with the other dimers. Surfactants are used for dispersing reactants in aqueous media. Sodium dodecyl benzene sulfonate (SDBS), a typical surfactant, was evaluated in the water medium (Fig. 2c). Even a half equivalent of SDBS decreased the conversion rate dramatically, and more equivalents of SDBS almost completely quenched the reaction. The cathode also substantially influenced the

https://doi.org/10.1038/s41467-024-52042-w

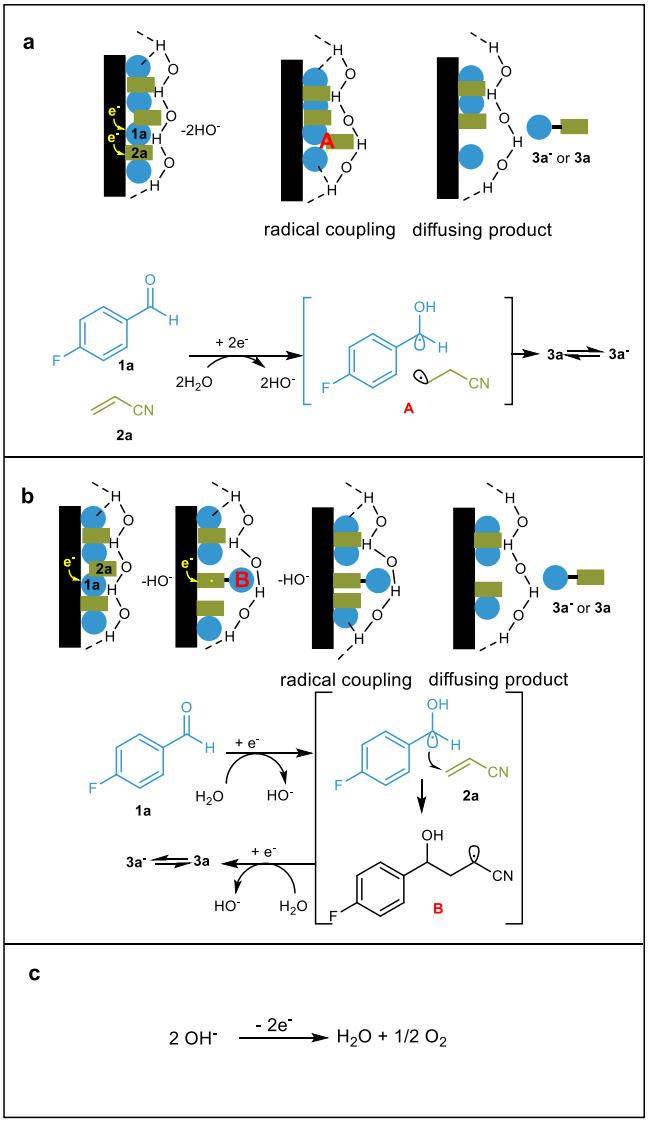

Fig. 4 | A plausible pathway involving aggregated substrates. a Two-electron-reduction pathway takes place at cathode. **b** One-electron-reduction pathway takes place twice at cathode. **c** The oxygen evolution at anode.

reaction (Fig. 2d). The graphite felt, which provided an adequate interface for aggregation, gave much better results than metals and carbon materials (see Supplementary Information, Section 2.2 for more details).

These results showed the substantial effect of aggregation, which led us to conduct additional investigations. First, the aggregated state of substrate **1a** on the cathode is shown in Fig. 3b for electrolysis for 10 s. Condensation of the substrate locally at the surface of the cathode was observed with aqueous media, but was not observed with MeCN as the solvent (Fig. 3c), which is similar to original material (Fig. 3a). This enrichment was confirmed by analyzing the mass distributions of the electrode and solution (Fig. 3d). For the water/GF electrode combination, approximately 90% of **1a** was aggregated at the electrode interface; in comparison, with organic solvents, the adsorption of **1a** on the surface of the electrode did not generate a significant imbalance (DMF 8%, MeCN 17%). Subsequently, the mass distributions of reactants **1a** and **2a** and product **3a** were measured in aqueous media (Fig. 3e). In contrast to aldehyde **1a**, acrylonitrile **2a** was soluble in water, which resulted in an average population. In addition, product **3a** showed better solubility than **1a** in water and did not aggregate significantly at the interface with the electrode. These differences led to a locally high concentration of **1a**, possibly due to the combined effects of the water tension and the lipophilicity of the electrode. We also measured the distribution of **1a** at graphite felt anode (Ti as cathode) and graphite felt cathode (Ti as anode) respectively in the absence of **2a** when the electrolysis was conducted for 10 min (Fig. 3f). It was found the graphite felt anode could adsorb 91% of **1a** and 9% of **1a** dispensed in aqueous media. In comparison, the **1a** was almost completely adsorbed on graphite felt cathode along with 23% of benzyl alcohol as the reduced product aggregated, and was almost not detected in aqueous media (<1%). Therefore, the aggregation was also influenced by the electric field effects significantly. This synergy effect brought the aggregated substrate closer to the interface with the electrode than it was in the organic solvent. To verify this hypothesis, we used cyclic voltammetry to study **1a** in aqueous media and in MeCN (Fig. 3g). Two clear differences were observed: (1) In aqueous media, the reduction of **1a** took place more readily, which supported the push-pull effect. (2) The peak current for 1a in the aqueous medium was lower than that in MeCN, possibly because of confined mass transfer in the aggregated environment. This confined mass transfer prevented dimerization of the radical intermediates observed in organic solvents. In comparison, water-soluble acrylonitrile exhibited a high current (Fig. 3h). This reduction potential and current profile implied that either a single reduction of **1a** or dual reduction of **1a** and **2a** might be possible. Therefore, a reaction was conducted with a controlled cathodic potential, and the dual reduction profile predominated (Fig. 3i). This dual reduction model was verified with radical trapping (Fig. 3j), which showed that both radicals were trapped by DMPO from the aggregated layer at the initial stage of the reaction using both HRMS and ERP analyses (5–15 min). Next, to determine whether the radical from **1a** was generated from the aggregated substrate or from the trace amount dissolved in water, a reaction employing a saturated solution of **1a** in water was carried out. Due to the poor solubility, no current or product was observed with identical electrochemical parameters (Fig. 3k). Alternatively, we used 1,4-benzenedialdehyde **1b** as a substrate and obtained product **3b** as the only cross-coupled product (Fig. 3l). This suggested that the aggregated aldehyde underwent the reaction, and product **3b**, which had higher solubility, diffused into the solution, and did not undergo electron transfer. Several kinetic features of this reaction were also evaluated (Fig. 3m). The yield of **3a** remained steady when the formal concentration of **1a** was changed from an experimental level (0.1 M based on the ratio of **1a**/water, but not a solution) to a productive level (1.0 M). Next, the influence of the current density on the conversion of **1a** was investigated (Fig. 3n). An increase in the current density did not lead to a significant increase in the conversion of **1a**. This observation prompted us to examine the influence of **2a** on the reaction (Fig. 3o). Unexpectedly, an increase in **2a** resulted in the consumption of only **2a**. In contrast, the conversion rate of **1a** decreased from 57% to 33%, suggesting that dimerization of **2a** was a major side reaction at high concentrations of **2a**. By tracking the conversion of substrate **1a** and the corresponding yield under standard conditions (Fig. 2), it was found that the chemoselectivity of the reaction continued to increase from the beginning and was almost complete in the aqueous medium (Fig. 3p). In contrast, with MeCN/water as a cosolvent, the chemoselectivity decreased, especially at high conversions (More details in Supplementary Information, Sections 2.4–2.7).

With these results, two plausible cathodic pathways were proposed (Fig. 4). For pathway 1 (Fig. 4a), two electrons were transferred to the aggregated aldehyde **1a** and acrylonitrile along with protonation by water, giving the two radicals adjacent to **A**. Subsequently, cross-coupling gives rise to product **3a**, which diffuses to aqueous media due to the difference in solubility between substrate 1a and product **3a**. In pathway 2 (Fig. 4b), one electron transfer with protonation occurs to give radical species **B**. A second radical transfer

https://doi.org/10.1038/s41467-024-52042-w

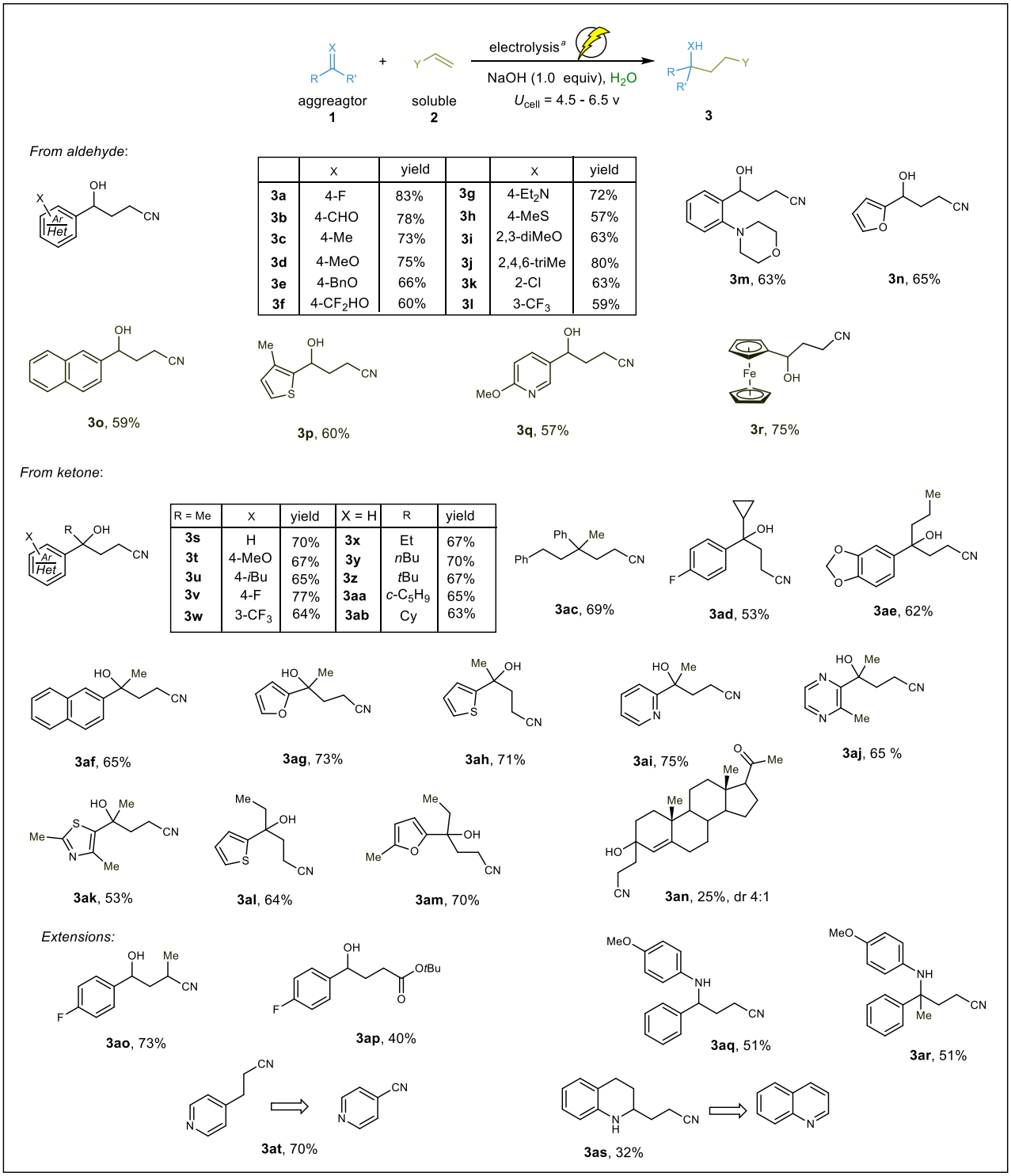

	X	yield		X	yield
3a	4-F	83%	**3g**	4-Et_2N	72%
3b	4-CHO	78%	**3h**	4-MeS	57%
3c	4-Me	73%	**3i**	2,3-diMeO	63%
3d	4-MeO	75%	**3j**	2,4,6-triMe	80%
3e	4-BnO	66%	**3k**	2-Cl	63%
3f	4-CF_2HO	60%	**3l**	3-CF_3	59%

R = Me	X	yield	X = H	R	yield
3s	H	70%	**3x**	Et	67%
3t	4-MeO	67%	**3y**	*n*Bu	70%
3u	4-*i*Bu	65%	**3z**	*t*Bu	67%
3v	4-F	77%	**3aa**	*c*-C_5H_9	65%
3w	3-CF_3	64%	**3ab**	Cy	63%

Fig. 5 | The substrate scope for electrochemical C–C bond construction. [a] Reaction conditions: **1** (0.4 mmol), **2** (0.8 mmol), NaOH (0.4 mmol), H_2O (5 mL), graphite felt anode and cathode; U_{cell} = 4.5-6.5 V under air for 4-11 h, isolated yields.

with protonation furnishes product **3a**. This product diffused into the solution and left the surface of the electrode open for substrate aggregation. At the anode, the oxygen evolution reaction occurred under basic conditions and provided a mass balance with oxygen as the only side product and a theoretical atom economy >82% (Fig. 4c). In such an aggregation state, the local electric field could have a more persistent effect on the aggregated species than under homogenous conditions and would be important to help with cross-coupling. Especially, due to the acid/base equilibrium, the existence of **3a**/**3a**$^-$/H_2O/HO^- could facilitate the diffusion of product, and more possibly its' anion to bulky phase.

This aggregation-driven radical cross coupling was exhibited with additional substances (Fig. 5). Various aromatic aldehydes underwent cross-coupling to the desired *g*-hydroxyl-nitriles **3a**-**3al** in decent to good yields. Furan, pyridine, and ferrocenyl groups were well tolerated. These ketones were also suitable for this reaction protocol. The g-tertiary alcohol nitriles **3s**-**3am** were synthesized in good yields. In particular, for product **3ad**, the radical cross-coupling reaction was

https://doi.org/10.1038/s41467-024-52042-w

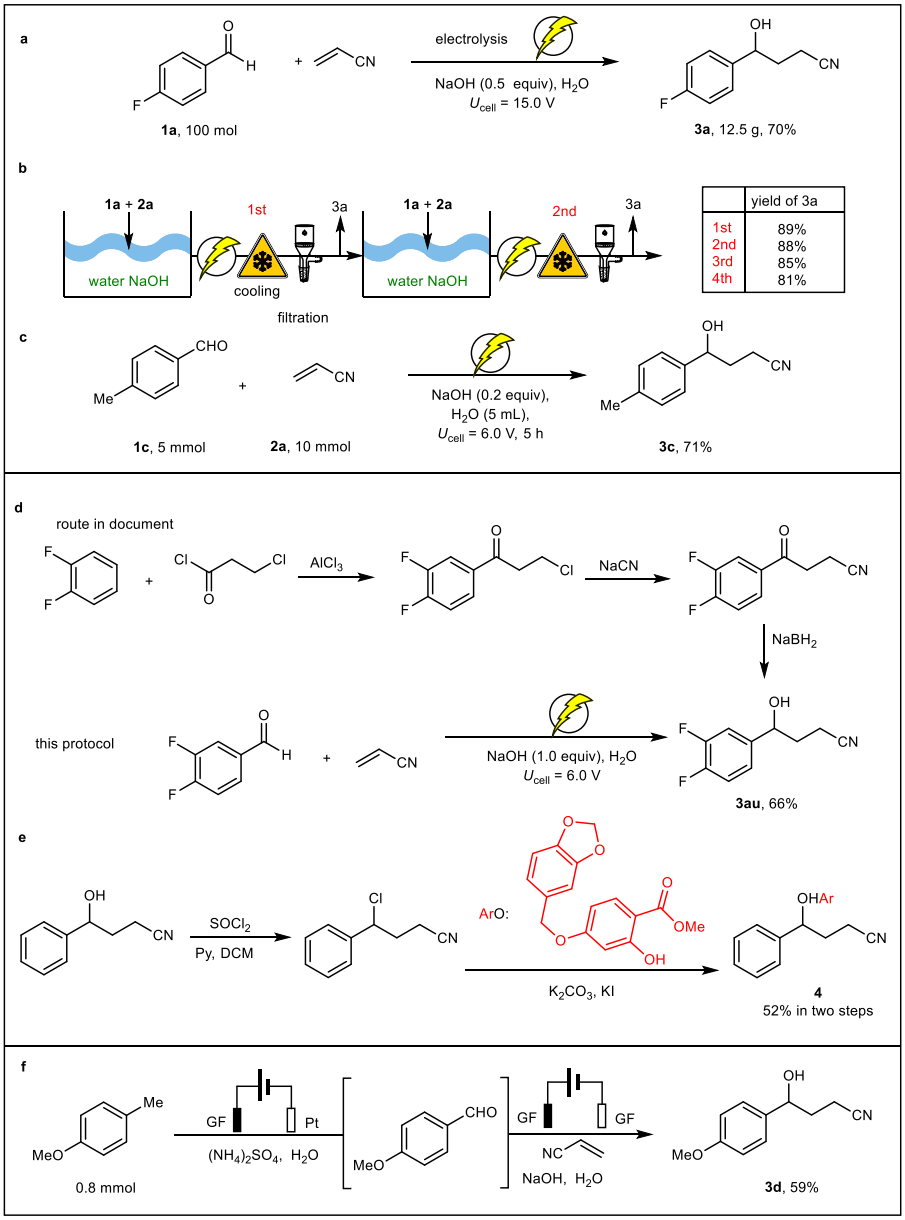

Fig. 6 | Additional applications of this aggregation-driven chemistry. a A standard reaction at dec-gram scale. **b** The recycle of water without any organic workup. **c** The reaction of 5 mmol **1c** in 5 mL water. **d** The synthesis of ticagrelor's intermediate **3au**. **e** The synthesis of endothelin antagonist **4**. **f** A tandem reaction in aqueous media.

faster than ring opening of the cyclopropyl group. The **3an** product from progesterone was obtained from a modified protocol with Cp_2TiCl_2 used as a catalyst. As an extension, the reactions of **1a** with *a*-methylacrylonitrile and *t*-butyl acrylate gave the corresponding products **3ao** and **3ap**, respectively, under standard conditions. In contrast to the readily hydrolysis in wet organic solvent, an imine substrate gave **3aq** as major product in 51% isolated yield under this condition. With the same manner, product from **3ar** ketimine was obtained in comparable yield. A tetrahydroquinoline **3as** was prepared from quinoline and **2a** in 32% yield. 4-CN-pyridine converted to compound **3at** in 70% yield.

Next, we demonstrated additional applications of this aggregation-driven chemistry (Supplementary Information, Sections 2.3, 2.8). A decigram scale reaction gave **3a** in 70% isolated yield (Fig. 6a). Recycling of the aqueous medium was evaluated by chilling the reaction mixture and using filtration to separate the organic product from water. The water was reused as a solvent, and the product was obtained with a comparable ^{1}H NMR yield of 88% (Fig. 6b). After three recycles of water media, the yield of **3a** remained high with adequate purity in crude NMR, and extraction with an organic solvent was not involved. The reaction of formal concentration of 1 M was conducted in 5 h, giving products **3c** in 71% yield (Fig. 6c). Next, the product **3au**, an intermediate for ticagrelor requiring a three-step route previously[37], was generated in 66% yield in single step (Fig. 6d). Similarly, the endothelin antagonist **4**[38] was synthesized with compound **3ao** as a building block with an overall 52% yield (Fig. 6e). The aqueous medium provided another advantage, as shown in Fig. 6f. 4-Methylanisole was oxidized in an acidic aqueous solution. In turn, by regulating the pH with added NaOH, product **3d** was obtained in a tandem process without workup and isolation.

Discussion

In summary, we demonstrated an aggregation effect during electrosynthesis. The tension of the water and the surface of the graphite felt constituted a push-pull combination. In this reaction, the substrate and, in turn, the poorly soluble radical intermediate was confined via aggregation, providing an opportunity for cross coupling of radicals

with good solubility. Another significant advantage of aggregation is the high chemoselectivities seen at high conversions, as the local high concentration at the electrode was maintained. This reaction reveals a model for electrochemical organic syntheses, including mass transfer, chemoselectivity, and reaction design.

Methods

General procedure for the synthesis of 3

To a 10 mL reaction flask was added 4-fluorobenzaldehyde **1a** (0.4 mmol,0.0496 g, 43 µL), and acrylonitrile **2a** (0.8 mmol, 2.0 equiv, 54 µL). NaOH (0.4 mmol, 0.016 g) in 5.0 mL H_2O was added as the reaction solvent. The reaction mixture was subject to electrolysis under 6.0 V constant voltage for 4 h with graphite felt as both anode and cathode. The color of reaction turned from colorless brown. Thin-layer chromatography analysis of reaction mixture showed the complete conversion was achieved. The reaction mixture was extracted with methylene chloride twice. The combined organic layer was dried (Na_2SO_4), filtered and concentrated. The residue was purified by silica chromatography with EA/PE = 1:5 (v/v) to offer **3a** as colorless oil.

Data availability

The authors declare that the experimental data generated in this study are provided in the Supplementary Information, and also are available from the corresponding author upon request.

References

1. Cai, X. & Liu, B. Aggregation-driven emission: recent advances in materials and biomedical applications. *Angew. Chem. Int. Ed.* **59**, 9868–9886 (2020).
2. Duo, Y. et al. Aggregation-driven emission: an illuminator in the brain. *Coord. Chem. Rev.* **482**, 215070 (2023).
3. Noël, T., Cao, Y. & Laudadio, G. The fundamentals behind the use of flow reactors in electrochemistry. *Acc. Chem. Res.* **52**, 2858–2869 (2019).
4. Lu, S. et al. Mass transfer effect to electrochemical reduction of CO_2: electrode, electrocatalyst and electrolyte. *J. Energy Storage* **52**, 104764 (2022).
5. Yan, M., Kawamata, Y. & Baran, P. S. Synthetic organic electrochemical methods since 2000: on the verge of a renaissance. *Chem. Rev.* **117**, 13230–13319 (2017).
6. Röckl, J. L., Pollok, D., Franke, R. & Waldvogel, S. R. A decade of electrochemical dehydrogenative C,C-coupling of aryls. *Acc. Chem. Res.* **53**, 45–61 (2020).
7. Novaes, L. F. T. et al. Electrocatalysis as an enabling technology for organic synthesis. *Chem. Soc. Rev.* **50**, 7941–8002 (2021).
8. Cheng, X. et al. Recent applications of homogeneous catalysis in electrochemical organic synthesis. *CCS Chem.* **4**, 1120–1152 (2022).
9. Wang, Y. L. et al. Electrochemical late-stage functionalization. *Chem. Rev.* **123**, 11269–11335 (2023).
10. Zeng, L., Wang, J. X., Wang, D. X., Yi, H. & Lei, A. W. Comprehensive comparisons between directing and alternating current electrolysis in organic synthesis. *Angew. Chem. Int. Ed.* **62**, e202309620 (2023).
11. Yin, Z. et al. CuPd nanoparticles as a robust catalyst for electrochemical allylic alkylation. *Angew. Chem. Int. Ed.* **59**, 15933–15936 (2020).
12. Li, H. et al. σ-Alkynyl adsorption enables electrocatalytic semihydrogenation of terminal alkynes with easy-reducible/passivated groups over amorphous PdSx nanocapsules. *J. Am. Chem. Soc.* **144**, 19456–19465 (2022).
13. Zhang, Y., Lin, Z. & Ackermann, L. Electrochemical C–H amidation of heteroarenes with N-Alkyl sulfonamides in aqueous medium. *Chem. Eur. J.* **27**, 242–246 (2021).
14. Li, R. et al. One-pot H/D exchange and low-coordinated iron electrocatalyzed deuteration of nitriles in D_2O to α,β-deuterio aryl ethylamines. *Nat. Commun.* **13**, 5951 (2022).
15. He, M. et al. Aqueous pulsed electrochemistry promotes C–N bond formation via a one-pot cascade approach. *Nat. Commun.* **14**, 5088 (2023).
16. Rusling, J. F. Green synthesis via electrolysis in microemulsions. *Pure Appl. Chem.* **73**, 1895–1905 (2001).
17. Wakisaka, M. & Kunitake, M. Direct electrochemical hydrogenation of toluene at Pt electrodes in a microemulsion electrolyte solution. *Electrochem. Commun.* **64**, 5–8 (2016).
18. Chiba, K., Jinno, M., Nozaki, A. & Tada, M. Accelerated Diels–Alder reaction of quinones generated in situ by a modified electrode in an aqueous sodium dodecyl sulfate micellar system. *Chem. Commun.* **15**, 1403–1404 (1997).
19. Nishimoto, K., Kim, S., Kitano, Y., Tada, M. & Chiba, K. Rate enhancement of Diels–Alder reactions in aqueous perfluorinated emulsions. *Org. Lett.* **8**, 5545–5547 (2006).
20. Nishimoto, K., Okada, Y., Kim, S. & Chiba, K. Rate acceleration of Diels–Alder reactions utilizing a fluorous micellar system in water. *Electrochim. Acta* **56**, 10626–10631 (2011).
21. Tian, C., Massignan, L., Meyer, T. H. & Ackermann, L. Electrochemical C–H/N–H activation by water-tolerant cobalt catalysis at room temperature. *Angew. Chem. Int. Ed.* **57**, 2383–2387 (2018).
22. Zhong, X. et al. Scalable flow electrochemical alcohol oxidation: maintaining high stereochemical fidelity in the synthesis of levetiracetam. *Org. Process Res. Dev.* **25**, 2601–2607 (2021).
23. Mikami, R., Shida, N. & Atobe, M. Integrated flow emulsion electrosynthetic system by in situ generation of emulsions, subsequent emulsion electrolysis, and final phase separation. *Org. Process Res. Dev.* **26**, 1268–1278 (2022).
24. Sun, Y. et al. Highly selective electrocatalytic oxidation of amines to nitriles assisted by water oxidation on metal-doped α-$Ni(OH)_2$. *J. Am. Chem. Soc.* **144**, 15185–15192 (2022).
25. Li, M., Cheng, X. Electrochemical organic synthesis in aqueous media. *Isr. J. Chem.* **64**, e202300067 (2023).
26. Marken, F. & Wadhawan, J. D. Multiphase methods in organic electrosynthesis. *Acc. Chem. Res.* **52**, 3325–3338 (2019).
27. Kitanosono, T. & Kobayashi, S. Synthetic organic "aquachemistry" that relies on neither cosolvents nor surfactants. *ACS Cent. Sci.* **7**, 739–747 (2021).
28. Shahid, M. Z., Usman, M. R., Akram, M. S., Khawaja, S. Y. & Afzal, W. Initial interfacial tension for various organic–water systems and study of the effect of solute concentration and temperature. *J. Chem. Eng. Data* **62**, 1198–1203 (2017).
29. Jiang, H. R., Shyy, W., Wu, M. C., Zhang, R. H. & Zhao, T. S. A bi-porous graphite felt electrode with enhanced surface area and catalytic activity for vanadium redox flow batteries. *Appl. Energy* **233-234**, 105–113 (2019).
30. Ruiz-Lopez, M. F., Francisco, J. S., Martins-Costa, M. T. C. & Anglada, J. M. Molecular reactions at aqueous interfaces. *Nat. Rev. Chem.* **4**, 459–475 (2020).
31. Yuan, Y. & Lei, A. Is electrosynthesis always green and advantageous compared to traditional methods? *Nat. Commun.* **11**, 802 (2020).
32. Cortes-Clerget, M. et al. Water as the reaction medium in organic chemistry: from our worst enemy to our best friend. *Chem. Sci.* **12**, 4237–4266 (2021).
33. Huang, X. et al. Methyl radical chemistry in non-oxidative methane activation over metal single sites. *Nat. Commun.* **14**, 5716 (2023).
34. Sun, S.-Z. et al. Enantioselective decarboxylative alkylation using synergistic photoenzymatic catalysis. *Nat. Catal.* **7**, 35–42 (2024).
35. Xu, Y. et al. A light-driven enzymatic enantioselective radical acylation. *Nature* **625**, 74–78 (2024).
36. Li, M., Zhang, T., Shi, Y. & Duan, C. Harnessing radicals in confined supramolecular environments made possible by MOFs. *Chem. Rec.* **23**, e202300158 (2023).

37. Zheng, Y. & Wu, Y. Green method for preparing ticagrelor and its intermediate thereof. Chinese patent, CN115894496A, applicant: Shanghai Bioman Pharma Ltd. (2023).
38. Cai, J. et al. Discovery of phenoxybutanoic acid derivatives as potent endothelin antagonists with antihypertensive activity. *Biorg. Med. Chem.* **23**, 657–667 (2015).

Acknowledgements

This work is supported by the National Science Foundation of China: 22471125, 22031008 and 22071105 to C.X. This work is supported by the Elite Student Development Program for Fundamental Disciplines 2.0: 20221021 to C.X.

Author contributions

L.M.F. conducted the experiments for reaction optimization, mechanism elucidation, and wrote the Supplementary Information. C.X. gave the reaction design and concept, and wrote the manuscript. L.M.F. and C.X. worked on the revision together.

Competing interests

The authors declare no competing interests.

Additional information

Supplementary information The online version contains supplementary material available at https://doi.org/10.1038/s41467-024-52042-w.

Correspondence and requests for materials should be addressed to Xu Cheng.

Peer review information *Nature Communications* thanks Kazuhiro Chiba, Bin Zhang and the other, anonymous, reviewer(s) for their contribution to the peer review of this work. A peer review file is available.